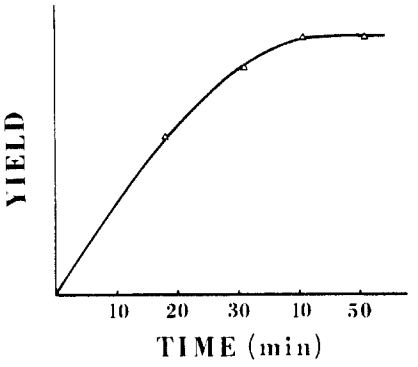

Figure 3. Yield of $C_2H_2I_2$ as a function of irradiation time. About 40 mW of 17012.09 cm^{-1} light was used.

within the first 20 min of reaction, where the curve is linear.

For a C_2H_2 pressure of 25 T, at the three dye laser frequencies (40 mW) and when using the Ar beam (200 mW), only the trans isomer was observed as a product. When the C_2H_2 pressure was varied from 5 T to 100 T and excited with the Ar laser beam at 200 mW, no cis isomer was observed. These results were confirmed by FTIR. The only reactions that yielded a trace amount of cis (3% or less of the trans isomer) were those excited with the Ar laser at 2.0 and 3.5 W for periods longer than 30 min. Previous publications had postulated the formation of the cis isomer by atomic addition under radiation at 488 nm.[8] Our results do not support such a hypothesis. In fact, no cis isomer was observed even when the photoreaction was induced at 325 nm with a HeCd laser with ~3 mW of power for 60 min. This suggests that the cis isomer is formed by a thermal, rather than photochemical process. Such a mechanism is consistent with the thermal conversion of trans to cis in the presence of iodine.[11]

Reaction of C_2H_2 with Isotopic Mixtures of Iodine. The dark and photochemical products, respectively, were analyzed by GC-MS to determine the isotopic composition before and after the selective excitation of a single isotope. Table II lists the results obtained together with the selectivity coefficients K, calculated as the ratio of the relative amounts of the isotopic species of interest after and before photoexcitation. The dark reaction is nonselective and thus the relative amounts give the initial isotopic composition of the reactants. This is a necessary measurement because the relative amounts of the three isotopic species of I_2 are difficult to determine directly at the start of the reaction, e.g., by selectively mixing the isotopic species of I_2. The quantities indicated as "photoproducts" represent the total amounts detected after the reaction minus the "dark" product extrapolated at the time of termination of the laser excitation. Such corrections are all 3% or less of the net photoproduct. In all cases the selectivity coefficient is near unity, indicating that scrambling occurs.

If the reaction proceeded by the addition of excited I_2 molecules to the C_2H_2 molecules, the K values would have been much greater than unity. So, we can conclude that the reaction occurs by addition of atoms to the C_2H_2 molecule. Furthermore, the severe scrambling observed indicates that such atoms do not come from the excited molecule only. Isotopic exchange in the gas phase or at the cell walls is known to be important.[7b]

Conclusions

The photochemistry of $I_2 + C_2H_2$ was reinvestigated by using single-frequency excitation, gas-phase product analysis, gas-phase FTIR identification of isomers, and GC-ECD and GC-MS measurements. Only trans $C_2H_2I_2$ is formed in the photochemical reaction regardless of excitation wavelength. *cis*-$C_2H_2I_2$ and -$C_2H_2I_4$ are formed as secondary reaction products, with the former going through a thermal, I atom assisted isomerization of the trans isomer. Gas-phase IR spectral band assignments reported here for *trans*- and *cis*-$C_2H_2I_2$ indicate that previous spectra[8a] are in error. Isotopic studies show complete scrambling in the products, confirming reaction by stepwise I atom addition. This implies that isotope separation of I_2 is not possible with this reaction scheme, in variance with earlier reports.[10] It seems that adsorption of I atoms on the walls of the reaction vessel is primarily responsible for a small degree of isotopic or ortho/para selectivity observed as the depletion of the species being excited. However, the low degrees of enhancement and the lack of a stable isotopic product precludes any practical utility.

Acknowledgment. The Ames Laboratory is operated for the U. S. Department of Energy by Iowa State University under Contract No. W-7405-eng-82. This work was supported by the Office of Basic Energy Sciences.

Registry No. C_2H_2, 74-86-2.

Some Tentative Models of Molecular Motion Applied to Water in Small Reversed Micelles

A. Llor* and P. Rigny

Contribution from the Département de Physico-Chimie, Commissariat à l'Energie Atomique, 91191 Gif sur Yvette Cedex, France. *Received July 31, 1985*

Abstract: The molecular dynamics of water in small, swollen, reversed micelles of sodium bis(2-ethyl-1-hexyl)sulfosuccinate (AOT) in cyclohexane has been investigated using proton NMR relaxation methods. When the water content drops from 15 to 3 molecules per AOT molecule, the ^1H NMR relaxation time T_1 is considerably reduced. This is due in part to slower motions of water molecules and also to the increased influence of external relaxation processes, such as the dipolar interactions with the surfactant protons. By progressive substitution of the micellized water by heavy water, the dipolar water-water effects have been distinguished from other relaxation processes. Using standard models of motion, this substitution has shown the water movements to be slower than in pure water by at most a factor of 5. This somewhat unusual result is in agreement with data from concentrated ionic solutions. The external relaxation effects displayed a frequency dependence which is typically induced by slow motions. Some dynamical models have been discussed to explain them, but the main effects seem to be induced by the dipole-dipole interaction with the protons of the AOT polar heads. The complex modulation of this interaction could not be described precisely, and a simplified model was used to deduce qualitative dynamical information from the experimental data. The water-polar head movements were then found to be in the range of 5×10^{-10} s.

For the last few years investigations on microemulsions and micellar systems have been greatly stimulated by possible applications in industry and in other scientific fields (biology, chemistry, etc.), as well as by the very specific phenomena these systems display. A reversed micellar system is a solution of spheroidal aggregates of amphiphile molecules in an aliphatic

0002-7863/86/1508-7533$01.50/0

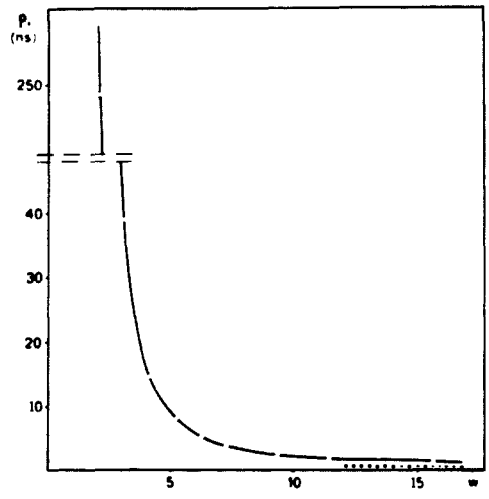

a) Variation in internal rotational relaxation time of PTC. The dashed line indicates the value measured in pure water.

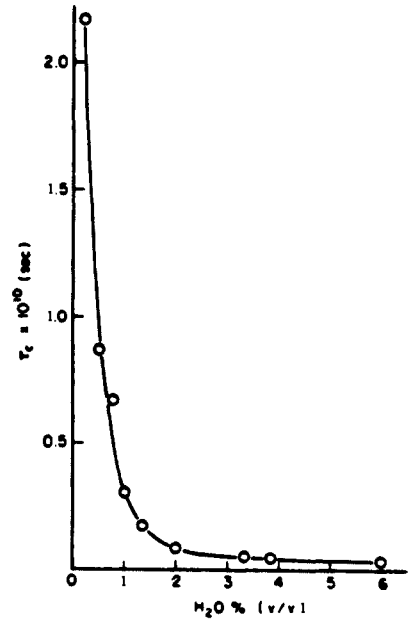

b) The effect of water content on the rotational correlation times τ_c, in 3% AOT/H_2O, C_7D_{16} reversed micelles

Figure 1. Typical graphics showing the dynamical behavior of water in reversed AOT micelles as a function of $W = [H_2O]/[AOT]$: (a) as seen by the fluorescence polarization decay of a probe added into the cores[2]; (b) as seen by NMR proton T_1 relaxation of the swollen water[3] (with permission of authors).

solvent. The hydrophilic polar heads point toward the center of the micelle in which some water can eventually be solubilized (swollen micelle). The stability of the aggregates is ensured by the molecular interactions (ionic, steric, hydrophobic effects,[1] etc.).

Most of the amphiphiles that are able to form inverse micelles are ionic and have double and branched aliphatic chains. The counterions and the water, if added, are confined in the micellar cores forming brine microdroplets of very high ionic strength. The properties of water in this environment are considerably different from those of pure water, and its dynamical behavior is of particular interest.

Although AOT (sodium bis(2-ethyl-1-hexyl)sulfosuccinate) is among the most widely used surfactants in industry and research for its high wetting and water-solubilizing properties, very few publications over the last few years deal with water microdynamics. In many of them, by observing (with EPR, fluorescence polarization decay, etc.) the reorientation of a probe added to the system, some dynamical information on water can be extracted, usually as an average viscosity parameter.[2] This semimacroscopic quantity depicts somewhat the microscopic motions, and usually increases with decreasing water content, W, defined as the molar ratio $[H_2O]/[AOT]$ (see Figure 1). This general behavior was supported by NMR proton relaxation measurements[3] which are apparently more reliable, particularly at small W as they do not need any probe addition. At $W = 6$, the water motions would thus be slower by a factor of $\sim$20 than in bulk water, according to these studies.

Meanwhile, a recent quasi-elastic neutron scattering experiment showed that much faster motions take place, even at low water content.[4] This seems to contradict the NMR results, as both techniques are sensitive to proton motions. But the NMR results were deduced from experimental data assuming that standard models of isotropic, continuous, and independent motions hold, and that the only relaxation source for water lies in the dipolar intramolecular interaction of water protons. The validity of these assumptions is far from obvious in the present case where complex motions in and of the aggregates take place.

The aim of this work is thus to study more closely water molecular motions as seen by NMR proton relaxation in the AOT reversed micellar system. To properly evaluate the water–water relative motions, the water–water dipolar proton relaxation was separated by progressive deuteration. The remaining relaxation displayed frequency effects, and some processes to explain it are discussed.

Experimental Method

AOT (Fluka purum) was purified according to a previously described procedure.[5] A stock solution of 0.1 M AOT was made by dissolving dry surfactant in deuterated cyclohexane (C_6D_{12}, from CEA, France, ref DMM17, enriched 99.5%). Mixing five equal volumes (measured with the same automatic micropipet) of heavy water (from CEA, enriched 99.5%) or deionized and purified water (Millipore system, 10 Mohm/cm), five different water enrichments x were made [x = 20, 40, 60, 80, and 100% H/(H + D)]. Four sets, each containing five samples of micellar solution of some W ratio, were then obtained according to the following procedure.

(i) In a 5-mm NMR tube the desired amount of water of the desired enrichment x was added with an automatic micropipet whose setting was not changed between samples of the same set. Although the water volumes involved were too small (about 20 μL) to have a very precise W (about 5%) from the micropipet, this ensured that all the samples of the *same set* had the *same W value*.

(ii) A 0.5-cm^3 portion of AOT stock solution was then added with the same micropipet for all the samples. The purpose of introducing the substances in this order was to "wash" the water eventually sticking to the tubes' walls, and thus promote a better W reproducibility between the samples.

(iii) The samples were then carefully degassed by the freeze–pump–thaw method (at least three times) and then sealed and shaken for homogeneity. The samples were stored in an air-conditioned room at 20 °C to equilibrate. All experiments were performed in the following month to avoid any degradation (AOT hydrolysis, for instance).

We measured the spin–lattice relaxation of the water protons using the standard inversion–recovery sequence at two different frequencies: 60.13 MHz on a Bruker WP 60 SY spectrometer, and 250 MHz on a Cameca TSN 250 spectrometer. A typical spectrum is shown in Figure 2. Because of partial overlap with the neighboring surfactant signals, the height of the water peaks used to fit the relaxation was estimated with

(1) Tanford, C. *The Hydrophobic Effect: Formation of Micelles and Biological Membranes*; Wiley: New York, 1980.
(2) Keh, E.; Valeur, B. *J. Colloid Interface Sci.* **1981**, *79*, 465.
(3) Wong, M.; Thomas, J. K.; Nowak, T. *J. Am. Chem. Soc.* **1977**, *99*, 4730.
(4) Tabony, J.; Llor, A.; Drifford, M. *J. Colloid Polym. Sci.* **1983**, *261*, 938.
(5) Pilēni, M.-P. *Chem. Phys. Lett.* **1981**, *81*, 603.

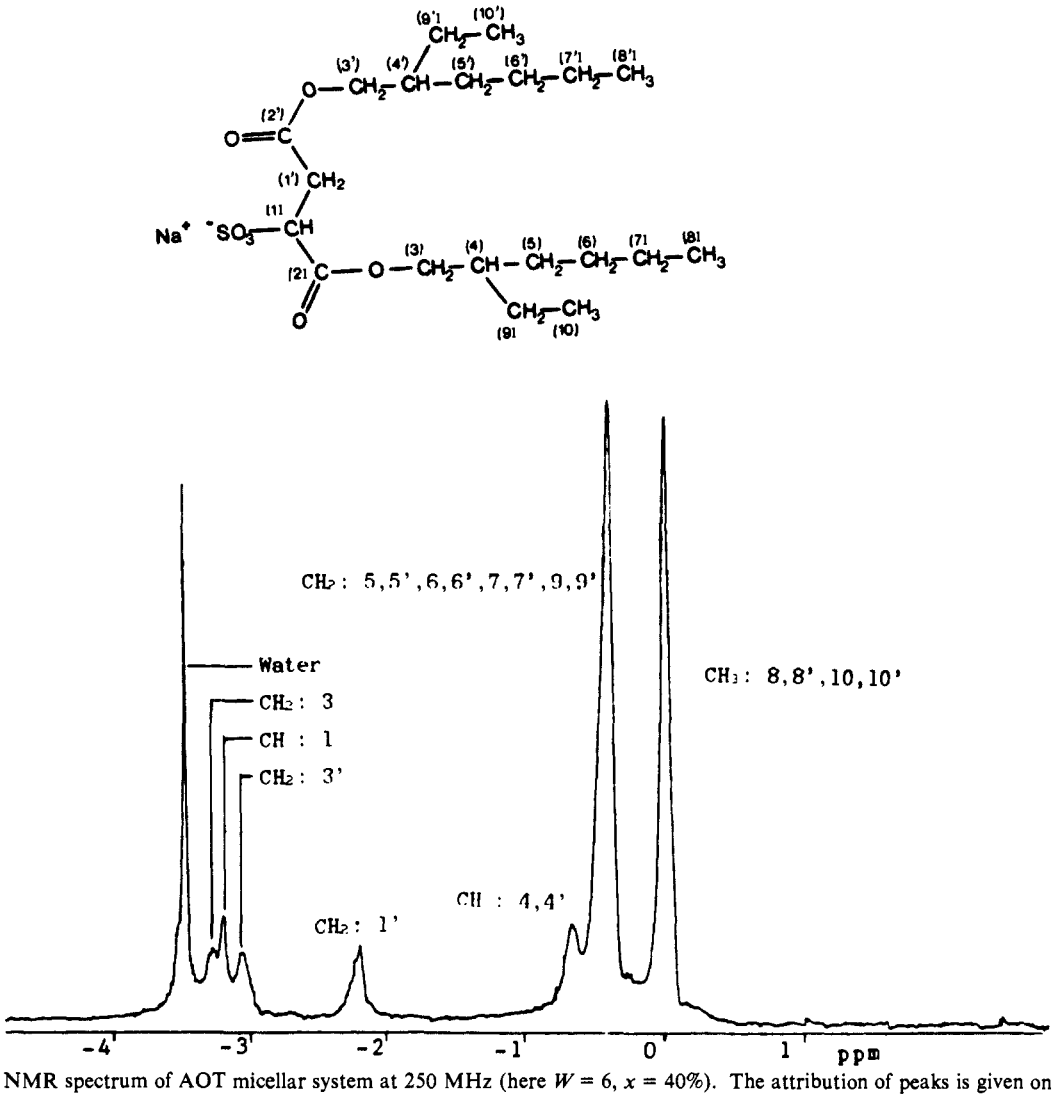

Figure 2. Typical NMR spectrum of AOT micellar system at 250 MHz (here $W = 6$, $x = 40\%$). The attribution of peaks is given on the developed formula.

some imprecision (particularly at low W and low frequency). We evaluate the average precision on T_1 to be around 5%. Nonexponential behavior of the relaxation was never observed within the experimental error. The results are summarized in Figure 3.

As already shown,[6] the water peak position is very dependent on W when $W < 15$, being shifted toward high fields as W decreases. Using the water signals' positions and integrals, we roughly checked the samples' compositions, discarding then two of them (which had probably lost some of their content during degassing).

Results and Discussion

(a) Water–Water Contribution. The hydrogen/deuterium substitution approach has already been applied to bulk water studies.[7,8] At room temperature the main relaxation effect arises from the modulation of the dipolar interaction between the nuclei due to the relative molecular motions. Other processes, like spin rotation or chemical shift anisotropy, are negligible for protons in this case.

In H_2O/D_2O mixtures, three chemical species are in equilibrium through a very fast exchange (about 10^{-11} s):

$$H_2O + D_2O \rightleftarrows 2HDO \qquad K = [HDO]^2/[H_2O][D_2O] \qquad (1)$$

The mixture is almost ideal and thus $K \simeq 4$. The observed relaxation is given by an average of all the relaxations over the different species and couples of nuclei (outer-sphere and inner-

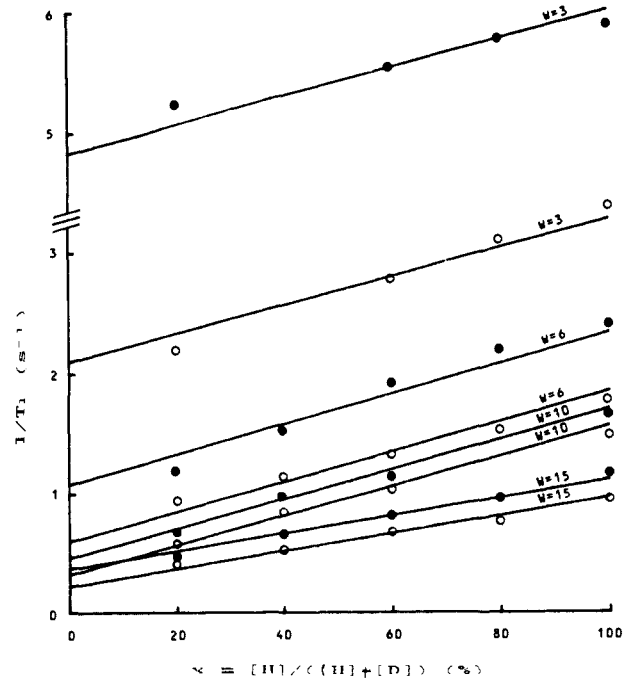

Figure 3. The experimental results $1/T_1$ plotted as a function of $x = 60$ MHz (full dots) and 250 MHz (empty dots) and at different water content, W. The straight lines are fitted according to the procedure described in text.

(6) Rouvière, R.; Couret, J. M.; Lindheimer, M.; Dejardin, J. L.; Marrony, R. *J. Chim. Phys.* **1976**, *76*, 289.
(7) Powles, J. G.; Smith, D. W. G. *Phys. Lett.* **1964**, *9*, 239.
(8) Smith, D. W. G.; Powles, J. G. *Mol. Phys.* **1966**, *10*, 451.

sphere terms, each being D over H or H over H). After some elementary algebra, the total relaxation in the ideal case is written as a function of $x = ([H_2O] + [HDO]/2)/([H_2O] + [HDO] + [D_2O])$, and of the relaxation rates of protons in pure water, $(1/T_1)_{100}$, and of a single proton in pure heavy water, $(1/T_1)_0$:

$$(1/T_1)_d(x) = x(1/T_1)_{100} + (1 - x)(1/T_1)_0 \quad (2)$$

Assuming that the molecular movements are not perturbed by the isotopic substitution, we have the relation:

$$(1/T_1)_{100}/(1/T_1)_0 = (3/2)(\gamma_H/\gamma_D)^2 I_H(I_H + 1)/I_D(I_D + 1) = 24 \quad (3)$$

This leads to:

$$(1/T_1)_d(x) = [(23x + 1)/24](1/T_1)_{100} \quad (4)$$

This law is not observed experimentally[7,8] and should be corrected from the molecular motions' modification with x. This has been done with the bulk viscosity of the mixture $\nu(x)$, which reflects on the macroscopic scale an average "slowing down" of the microdynamics. When using $(1/T_1)/\nu(x)$ instead of $1/T_1$, eq 4 fits the experimental data. The nonideality of the mixture is too small to have any measurable effect on this behavior.

In the present experiment, this approach can be used in the same way with the same eq 1 to 4 for the relaxation fraction induced by all the water protons of the micellar core. The following assumptions are also required.

(i) Fast Exchange and Extreme Narrowing: The relaxation of water as noted in ref 3 does not display any drastic change but a continuous evolution when W varies from 0 to very high values (around 40), where the water behaves very similarly to bulk water. Otherwise, there would be a the slowing down of motions to such an extent (over the Larmor frequency) that the average equation (2) would not be valid any more.

(ii) Quasi-ideality of the H_2O/D_2O Mixture: This fact cannot be easily tested, but there is no reason to expect the ideality of water in the micellar core to be different from that of bulk water.

(iii) Viscosity Influence Correction: Since no viscosity data exist for water/heavy water mixtures inside the micellar cores, we have neglected this correction, which is probably smaller than in bulk water because of the lower hydrogen bond rate and of the strong influence (independent of x) exerted by the ions in the water pool. This approximation is supported by the fact that the heavy water to light water ratio of viscosities displays a standard weight behavior (about 20/18) at high temperatures, while at low temperatures the peculiar isotopic effects on the hydrogen bonds raise the viscosity difference to unusualy high values (about 25%).[9] In many H/D substitution experiments on "simpler" liquids like benzene,[10] the isotopic effect on viscosity (which is reduced to the weight effect) is neglected and the results are not significantly affected.

Using formula 4, straight lines were fitted by the least-squares method through the plot of experimental $1/T_1$ vs. x (without any viscosity correction). At each frequency, and for each same W set of samples, this gave two parameters, as shown in Figure 3: the slope of the line, which is the relaxation due to water protons on water protons, and the y intercept, which is the relaxation due to all the other relaxation effects. These quantities will be qualified from now on as "inside" and "outside" contributions, respectively.

The first property of the "inside" relaxations that we want to stress is their frequency independence. At 60 and 250 MHz the "inside" values are identical within experimental error for all the chosen W values, whereas the "outside" contributions differ substantially. Using this property to enhance precision and coherence, the experimental results were fitted again at each W value with the constraint of "inside" relaxation equality at 60 and 250 MHz. The results are listed in Table I, corrected from the 1/24 term of eq 4.

Table I. Experimental Water–Water and Water–Surfactant Relaxation Rates of Water in AOT Micelles of Different W Ratios[a] and Deduced Correlation Times for the Water Molecular Movements[b]

water content W	3	6	10	15
water–water, $1/T_1$ (in s^{-1})	1.22	1.30	1.29	0.78
water–AOT, $1/T_1$ at 60 MHz	4.78	1.03	0.41	0.34
water–AOT, $1/T_1$ at 250 MHz	2.05	0.55	0.27	0.19
correlation time (in 10^{-11} s)	1.10	1.18	1.17	0.70
correlation ratio to pure water	3.7	3.9	3.9	2.3

[a] Corrected from the 1/23 term; see eq 4. [b] Using $\rho = 1$ in eq 6.

The interpretation of the relaxation can be drawn in terms of nuclei motions after stating some hypotheses. Those usually assumed for bulk water can be completed for micellized water.

(i) The only efficient movements are molecular reorientations and mutual diffusion of the molecules, considered as dimensionless points. Vibrational and eccentricity effects are supposed to be negligible.

(ii) All the movements (inter and intra) are described by continuous and isotropic diffusions. This is well-verified in NMR, where the time scale is long compared to molecular motions in liquids. No evidence for jump diffusion or quantified motion effects on NMR has ever been recorded in water.

(iii) Furthermore, in the micellar case, the translational diffusion is confined in a restricted media and is affected by water exchange between micelles. Now, in all the cases we studied, the micellar core size (~20 Å) is considerably larger than the closest approach distance between the molecules; the relative self-diffusion can be considered as unbounded for all the molecules, except for those in the thin layer on the core surface, which have small relative importance. Water exchange between micelles has no influence, since it happens mostly in micelle–micelle collisions[11] whose time scale is very long compared to the intramicellar and NMR time scales.

(iv) The movements are correlated and perturbed by the presence of ions and polar heads as well as by collective effects (like overall aggregate motion). Meanwhile, the water movements average out the dipolar interaction and are much faster than all the other characteristic movements whose influence is thus negligible on the T_1 homonuclear relaxation (they can be considered as frozen).

(v) The characteristic time constants for both movements (rotational (intra) and translational (inter)) are identical $\tau_r = \tau_1 = \tau$. Although this is probably the most questionable statement, fast proton exchange in water makes NMR unable to discriminate the movements (contrary to what can be done in other liquids[10]). Other experimental techniques (like Kerr effect relaxation, or ^2D NMR relaxation) have given some support to this point, at least in orders of magnitude for bulk water. In any case, and particularly in the micellar system, the global correlation time represents a linear combination of τ_r and τ_1.

(vi) All the movements are in the extreme narrowing limit, $\omega\tau << 1$. This is well-known for water and, as we mentioned previously, still stands for micellized water.

Under these assumptions the relaxation rate due to water protons can be written in the extreme narrowing limit as:[12]

$$(1/T_1)_i = (3/2)\gamma^4\hbar^2(1/d^6 + (\pi/15)\rho/a^3)\tau_i \quad (5)$$

where ρ is the proton density in water, $d = 1.516$ Å is the interproton distance in the water molecule, and $a = 1.38$ Å is the pseudo-closest approach distance for water molecules. This gives numerically:

$$(1/T_1)_i = (6.95 + 4.10\rho) \times 10^{10}\tau_i \quad (6)$$

(time units being seconds and ρ standing now for the relative density of water).

(9) Heicks, J. R.; Barnett, M. K.; Jones, L. V.; Orban, E. *J. Phys. Chem.* **1954**, *58*, 488.
(10) Powles, J. G.; Figgins, R. *Mol. Phys.* **1966**, *10*, 155.
(11) Atik, S. S.; Thomas, J. K. *Chem. Phys. Lett.* **1981**, *79*, 351.
(12) Powles, J. G. *Relaxation Processes*; The Chemical Society: London, 1966.

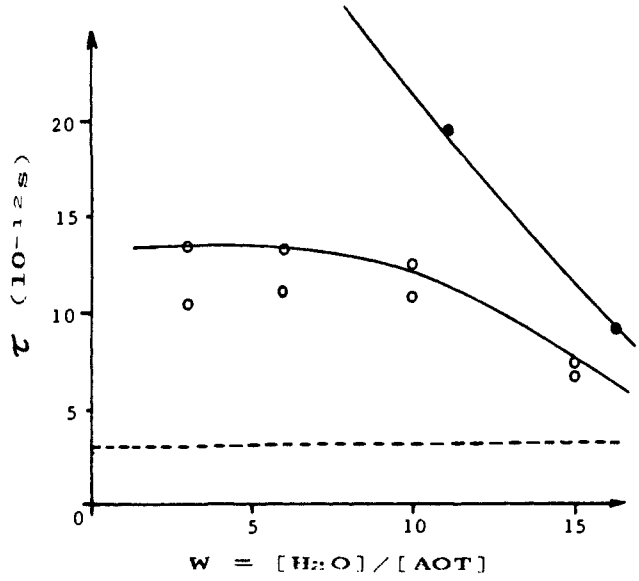

Figure 4. The water molecule correlation time in AOT micelles as a function of W shows the motion slowdown as W decreases. The lower points were obtained with a unity water density in the micelles, whereas for the upper points the counterions and polar head volumes were taken into account in eq 6. The line on the upper right corner was drawn from data in ref 1. The dotted line is the value found in pure water at the same temperature.

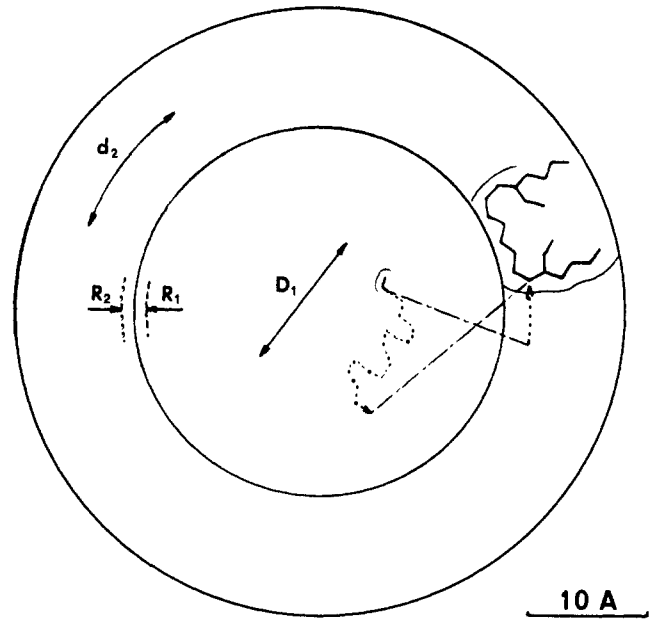

Figure 5. On-scale schematic drawing of a $W = 6$ AOT micelle showing how local fast motions can induce a slow modulation of long-range dipolar interactions between water and surfactant. Radii R_1 and R_2 and diffusion constants D_1 and d_2 are used in the calculation of this effect. The surfactant shell is assumed to be "dry"; all the water is packed in the central spherical core. The simplified skeleton (reduced to the aliphatic and ester chains of AOT) illustrates the mean size and conformation of the surfactant in the shell.

As a first approach, using $\rho = 1$ in eq 6, the experimental corrected "inside" data give the water correlation times τ_i, as listed in Table I and also plotted in Figure 4. When W decreases, τ_i increases and then seems to stabilize for $W < 10$, with even a slight decrease. This last and unexpected property is probably due to the fact that ρ is smaller than 1 in the micellar core (the correction is done in the following section). In any case, the maximum τ_i value stands at about five times its pure water value. This result, at variance with previous estimates,[3] has been obtained through our use of the isotopic substitution method; it reconciles studies on water in reverted micelles with known properties of water in concentrated ionic solutions, previously studied by NMR.[13]

(b) "Outside" Contributions: A Tentative First Explanation. The "outside" relaxation contains all the relaxation effects other than the dipolar interaction modulation between the water protons. Many processes must a priori be considered, but we will discard most of them.

(i) It has been proved[8] that spin–rotation coupling effect is negligible at ambient temperature for water, and the demonstration is easily extended to our case.

(ii) The chemical shift anisotropy modulation on H nuclei has also been quoted.[3] As far as we know it has never been observed in similar cases, and seems unlikely to ever be, since the chemical shift anisotropy of protons as measured in ice is to small (about 30 ppm) and since water bonding with the Na^+ or SO_3^- ions should not induce any extra anisotropy.

(iii) The dipolar coupling modulation with other present nuclei is negligible compared to the influence of the protons of the AOT layer. An elementary calculation shows,[18] for instance, that the Na^+ contribution is a few percent of that of the AOT protons, assuming an equivalent motion in both cases (this is even an overestimation, the surfactant movements being much slower and closer to the Larmor frequency than those of sodium, thus inducing a much stronger relaxation).

(iv) The influence of uncontrolled paramagnetic impurities has to be considered since the purity of the surfactant in this respect is very difficult to check. Anyway, the purity of the various compounds, the careful purification procedure, as well as the degassing will be considered to have minimized the relaxation from eventual paramagnetic species. Besides, the relaxation induced by paramagnetic ions never displays any significant frequency dependence above 5 MHz,[19] unless the ions have long electronic relaxation times and their hydration spheres have long reorientation times and mean lives.

Thus the only efficient "outside" relaxation process left in this system can be found in the dipolar interaction modulation between the surfactant and water protons. Most noticeably, the "outside" relaxation times are frequency dependent. As in all the systems which display such a property, this can be explained by assuming the dipolar modulation to be slower than the Larmor frequency. Though the motion of the individual water molecules is fast, a slow angular modulation of the dipolar interaction may arise with the surface where the surfactant is confined (from far enough a fast local motion is seen as slow, Figure 5). An elementary calculation shows, for instance, that the average time needed for a water molecule to diffuse over a distance equal to the micellar core diameter is close to the characteristic Larmor time $1/\omega$ (assuming the water self-diffusion constant to be less by a factor of 5 than in pure water, and the micellar core size as already given[14]).

In order to evaluate accurately the relaxation induced by the back and forth movement of water in the micellar core, an exact spectral density calculation was developed. The detailed calculation uses a two-particle ideal model[15,16] integrated over the core and shell of protons as given in the Appendix. We will recall the assumptions and results needed in the present case.

(a) The aggregates have spherical symmetry. (b) The average sizes of the core and the whole aggregate are deduced using the aggregation number of monomers, N, as given for each W value by Day et al.,[14] and the mean molecular volumes of water and AOT[6] (see Table II).

(c) The proton distribution is uniform in the shell and the core. The density in the shell, N_2, is 60 protons/nm^3 (this is the average value for aliphatic compounds).

(13) Boden, N.; Mortimer, M. *J. Chem. Soc., Faraday Trans. 2* **1978**, *74*, 353.

(14) Day, R. A.; Robinson, B. H.; Clarke, J. H. R.; Doherty, J. V. *J. Chem. Soc., Faraday Trans. 2* **1979**, *75*, 132.

(15) Llor, A. Note CEA N-2382 (Thesis work), Commissariat à l'Energie Atomique, France, 1984.

(16) Llor, A.; Rigny, P., to be published.

Table II. Water Protons–Aliphatic Protons Cross-Relaxation Rates (in s^{-1}) Induced by the Surfactant Shell Protons as Estimated with Eq 8 to 11 at 60 and 250 MHz as a Function of W[a]

water content, W	3	6	10	15
aggregation number	47	86	127	160
water pool radius (Å)	10.0	15.5	20.8	25.8
aggregate radius (Å)	20.3	25.7	30.7	34.8
τ_1, water cor. time in pool (10^{-9} s)	1.5	3.8	6.8	6.2
τ_2, AOT cor. time around pool (10^{-9} s)	57	116	197	287
R_{11} at 60 MHz	0.18	0.11	0.08	0.05
R_{12} at 60 MHz	−0.04	−0.02	−0.007	−0.007
R_{21} at 60 MHz	−0.007	−0.005	−0.004	−0.006
R_{22} at 60 MHz	0.03	0.04	0.04	0.04
R_{11} at 250 MHz	0.14	0.08	0.06	0.04
R_{12} at 250 MHz	−0.06	−0.03	−0.02	−0.01
R_{21} at 250 MHz	−0.01	−0.01	−0.01	−0.01
R_{22} at 250 MHz	0.02	0.03	0.03	0.03

[a] The geometrical and dynamical parameters used in this evaluation are listed as well.

(d) The water motion is properly described by a uniform diffusion confined to a sphere which is a model of the micellar core.

(e) The translational diffusion coefficient of water inside the core, D_1, is given relative to its bulk water value, by the corresponding ratio of the correlation times deduced in the preceding section.

(f) The shell of aliphatic protons is considered as a solid, the movements of the nuclei being only those of the whole aggregate. This neglects the local chain motions (which are ineffective on a long range modulation), as well as the lateral diffusion of the surfactant on the surface. This last motion is not known precisely but can be estimated from previous NMR–pulse gradient spin echo experiments on liquid-crystal phases of AOT.[17] Assuming a lateral diffusion constant of about 10^{-7} cm^2/s on the surface, the total reorientation of the AOT molecules around the micelle is dominated by the reorientation of the whole aggregate. Furthermore, the individual and collective motions on the micelle cannot be distinguished since they produce identical behavior of the NMR relaxation in the core, as shown elsewhere.[15,16]

(g) The effective rotational diffusion constant is roughly evaluated through the Stokes–Einstein formula:

$$d_2 = kT/8\pi\eta R_a^3$$

where R_a is the radius of the aggregate and η the viscosity of the solvent. η was estimated from its value in C_6H_{12}, 0.96 cP, scaled by the density ratio of heavy to light solvent (R_a is quoted in Table II).

(h) Water and surfactant diffusions are independent. The sole correlation between them stands in their bounding to the same aggregate.

(i) The distance of closest approach between an aliphatic proton and a water proton is 2.1 Å. As the water core diameter is the limit between the van der Waals bonds of the water and aliphatic molecules, the confinement radii for the nuclei, R_1 and R_2, are thus 1.05 Å on each side of the core radius (reported in Table II).

(j) The protons of the shell behave as a set of identical spins (the CH_2 signals give a single wide line due to their number and to the efficiency of their relaxation). This means that the general set of crossed relaxation equations can be properly integrated over the surfactant distribution of protons to yield a reduced set of two linear equations:

$$\frac{d}{dt}\begin{pmatrix}M_1\\M_2\end{pmatrix} = \begin{pmatrix}R_1 + R_{11} & R_{12}\\R_{21} & R_2 + R_{22}\end{pmatrix}\begin{pmatrix}M_1 - M_{10}\\M_2 - M_{20}\end{pmatrix} \quad (7)$$

where indexes 1 and 2 stand for the water and surfactant magnetizations, respectively.

(17) Lindblom, G.; Wennerstrom, H. *Biophys. Chem.* **1977**, *6*, 167.

As standard relaxation models show,[18] the dipolar contributions to the relaxation rates, R_{ij}, can be written:

$$R_{11} = (8\pi/5)(\gamma_1\gamma_2\hbar)^2 I_2(I_2 + 1) \times [J_1(\omega_2 - \omega_1)/3 + J_1(\omega_1) + 2J_1(\omega_1 + \omega_2)] \quad (8)$$

$$R_{12} = (8\pi/5)(\gamma_1\gamma_2\hbar)^2 I_1(I_1 + 1) \times [-J_1(\omega_2 - \omega_1)/3 + 2J_1(\omega_1 + \omega_2)]$$

with the symmetrical relations for R_{22} and R_{21}. J_1 and J_2 are the spectral densities integrated over the proton distributions which are given, under the above assumptions, by series of Lorentzian functions (see Appendix):

$$J_1(\omega) = N_2/R_2^3 \sum_{l,\,n=0}^{\infty}\sum B_{ln}\tau_{ln}/(1 + \omega^2\tau_{ln}^2)$$
$$J_2(\omega) = (2W/37)J_1(\omega) \quad (9)$$

with the reduced amplitudes:

$$B_{ln} = [(l + 2)(l + 1)l^2]/[u_{ln}^2(u_{ln}^2 - l(l + 1))] \times (R_1/R_2)^{2l}[1 - (R_2/R_a)^{2l+3}] \quad (10)$$

The τ_{ln} are functions of the correlation times of the individual particles:

$$1/\tau_{ln} = u_{ln}^2/\tau_1 + 6/\tau_2 \quad (11)$$

$$1/\tau_1 = D_1/R_1^2,\ 1/\tau_2 = d_2 \quad (12)$$

and the u_{ln} are the n-labeled solutions of the l-labeled equations $j_l'(u_{ln}) = 0$ (j_l' is the derivative of the lth order spherical Bessel function), which arise when solving the eigenvalue equation for the diffusion operator of particle 1.

Although these equations seem rather heavy, they are very easily implemented on microcomputers for simulation. The series converge rapidly, and one can drop the terms with large enough values of l and n without significant error. A table of the first u_{ln} values (from literature[15] or from computation) can be stored once on a mass memory for use in all the simulations.

Using eq 9 to 12 in the relaxation formulas 8 (with parameters R_1, R_2, D_1, d_2, and N_2 as given in points i, e, g, and c), one can calculate the contributions to the "outside" relaxation due to the shell-core nuclear interactions at the experimental frequencies, 60 and 250 MHz. It is clear that the results of the calculation, listed with τ_1 and τ_2 in Table II, are at best about an order of magnitude smaller than the experimental values, showing failure of the considered model. Either the relaxation process we have considered is not the main one, or some of the assumptions about our system are wrong.

Even though the long-range relaxation scheme discussed here turns out not to be effective, it must be pointed out that it was not a priori possible to discard it. The smallness of the calculated relaxation effects is due mainly to the dynamical factors that we were forced to introduce. All other parameters keeping the same values, one can find values of D_1 and d_2 which give calculated relaxation rates comparable to the experimental rates. This is shown in Figure 6 by the contour plots of the quantities R_{11} and $R_{11} + R_{12}$ as functions of the correlation rates τ_1 and τ_2, all other parameters being those of a $W = 6$ micelle. R_{11} is the relaxation rate induced on water when the aliphatic protons have a strong self-relaxation rate R_2, and $R_{11} + R_{12}$ represents the global energy transfer rate between the spin system and the lattice. An increase by about an order of magnitude in the calculated relaxation rates may be reached by changes of an unrealistic magnitude in the correlation times τ_1 and τ_2 and their associated diffusion constants evaluated in points e and g.

The calculation summarized here is a rigorous one for an often-invoked relaxation mechanism; even if, after all, not operant here, one can think of many physico-chemical situations where it has to be considered.

(c) Effects of Interface Adsorption: The Actual Relaxation Mechanism. Still assuming that the relaxation primarily originates from the AOT protons, it must be concluded that some of the

(18) Abragam, A. *The Principles of Nuclear Magnetism*, Clarendon Press: Oxford, 1960.

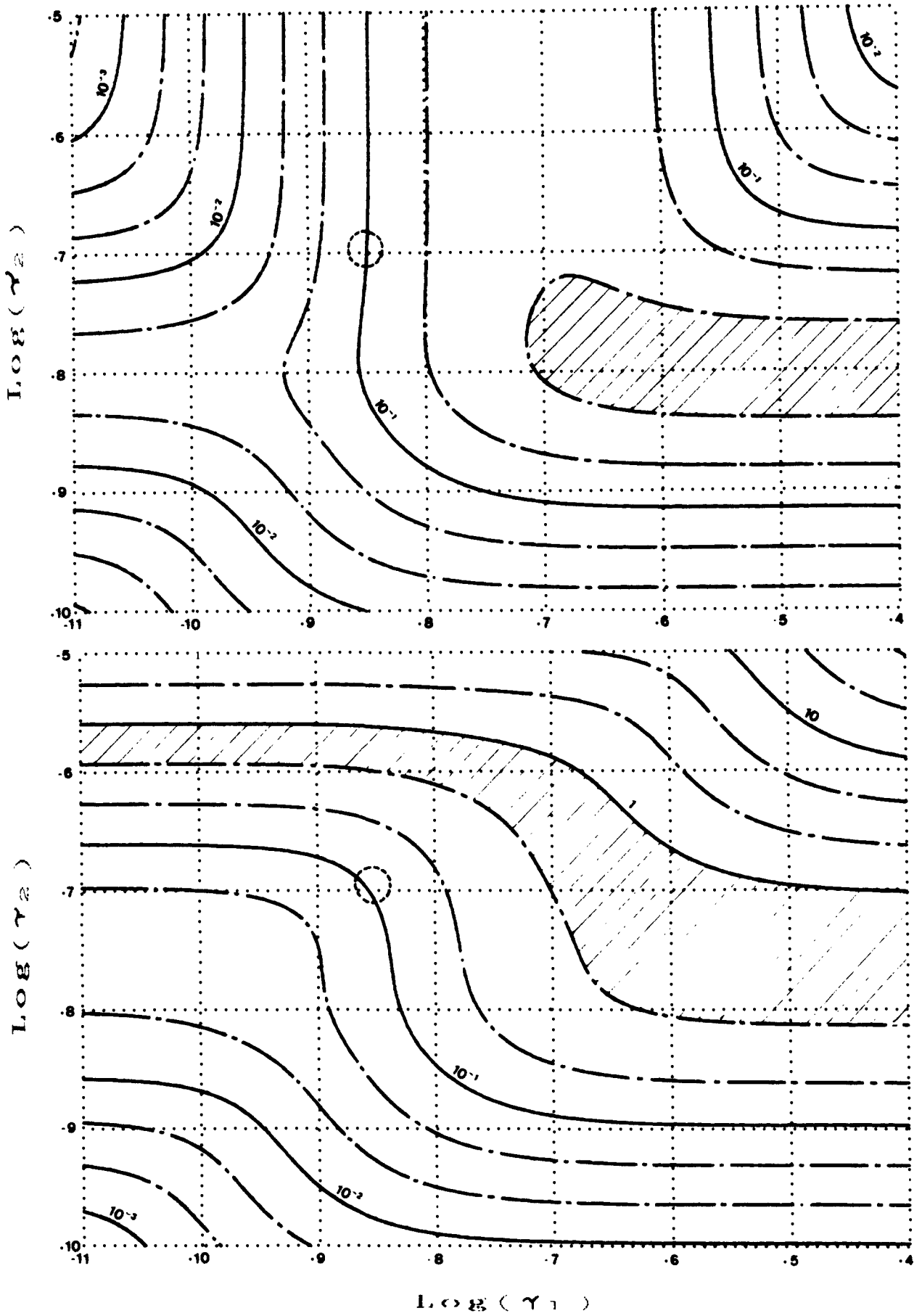

Figure 6. Logarithmic contour plots of the cross-relaxation quantities $R_{11} + R_{12}$ (global relaxation rate between spins and lattice) and R_{11} (effective relaxation induced on water by the AOT shell assuming fast self-relaxation of the surfactant protons) as functions of the correlation times τ_1 and τ_2 (see Figure 5) and eq 7 to 12). The geometry is assumed to be that of a $W = 6$ AOT micelle. In the hatched regions the calculated and experimental relaxations are of similar magnitude but are much too far (about 1 to 2 orders of magnitude) from the actual estimated values of τ_1 and τ_2 indicated by the dotted circle spot. Similar situations are also found for the other explored W values.

Table III. Corrected Water Molecular Correlation times, τ_i[a]

water content, W	3	6	10	15
ionic pool radius (Å)	13.4	18.4	23.4	28
"dry" AOT head thickness (Å)	3.4	3.0	2.6	2.2
water rel density in pool	0.42	0.59	0.71	0.78
τ_i, water cor. time (10^{-11} s)	1.41	1.39	1.31	0.77
τ_i, ratio to pure water	4.7	4.6	4.4	2.5
τ_0, water–head cor. time (10^{-9} s)	0.66	0.50	0.34	(0.47)
r_{eff}, mean eff distance (Å)	2.5	3.1	3.5	3.7

[a] Taking into account the effective water density in the core. The "outside" relaxation rates give the correlation time for the relative water–AOT polar head interaction τ_0 and its mean effective distance r_{eff} according to the qualitative procedure described in section c. The value in parentheses is subjected to an estimated 50% experimental error due to the extrapolation procedure used to get the "outside" relaxation rates.

assumptions in the previous model are wrong. Since an order of magnitude effect on the relaxation is needed, most of the hypotheses can be discarded, except the stiff step boundary assumption between water and surfactant which is implicitly cited in points d, h, and i (a detailed discussion can be found in ref 15). Actually the water–surfactant interface is very diffuse, with water molecules adsorbed in the polar head shell. Elementary considerations using the mean molecular volumes of water, AOT, and aliphatic chains provide support to this picture.

Using the mean density of aliphatic chains, 0.713, one can deduce the radius of the polar head shell as listed in Table III. If the polar heads are "dry", all the water in the micelle is confined in the core whose radius already calculated gives the thickness of the layer. Table III shows the layer thickness is about 3 Å for small micelles, and close to 2 Å in the high W range. An elementary evaluation (with ball models for instance) shows that it is not possible to accommodate the whole AOT polar head (two esters, one sulfonate on a four-carbon skeleton) in such a thin layer; the water molecules have thus to be partially adsorbed in the layer between the AOT polar heads. This is, in fact, no great surprise and it is even probable that in small micelles there no longer exists any free water core but a sole ionic core of mixed polar heads, counterions, and water.

The amount of adsorbed water can be evaluated from the τ_i behavior with W. Assuming that it is independent of the water pool size, and that the water in and out of the ions and polar head hydration spheres is described by a standard pseudo-phase model,[19] $1/\tau_i$ is an average value over the two regions. Since τ_i is almost constant against W up to $W_0 \simeq 8$ to 10, the amount of water in the hydration spheres can be estimated to be around W_0 molecules per polar head. Considering that the sodium ion has five to six water molecules in its hydration shell,[19] there are three to four water molecules per AOT adsorbed in the shell of the polar heads. Other techniques have given estimates of W_0; X-ray small angle scattering[20] provides a 15 to 16 value. Since the electronic density contrast to which it is sensitive arises primarily from the shell of polar heads *and* of Na^+ counterions, the X-ray value is compatible with a smaller NMR value. Similar conclusions can be drawn from fluorescence yield measurements of probes dissolved in the water pools.[21]

In this environment, the mean distance between water molecules is larger, thus reducing the "inside" relaxation, whereas the vicinity of the polar head protons becomes a major source for the "outside" relaxation. The later is then more intense than in our previous model and is no longer influenced by "long-range" effects.

Let us examine the "inside" part. Fast water exchange in the micellar core averages the effects of adsorption in the polar heads; this is given in eq 5 by a smaller ρ value (the mean distances between water molecules are larger). Although we do not know precisely the density effect of the process, we can give a lower bound to ρ assuming the water molecules are scattered over the whole "polar heads + water" core (this is the limiting case of a unique "ionic" core as already described). Using the calculated radius for the polar head shell, we obtained the new values of ρ and τ_i, as listed in Table III and also plotted in Figure 4. One sees that the new τ_i behavior with W is now monotonic, which seems more relevant.

The polar head contribution to the "outside" relaxation is expressed through coupled equations like (7), in which index 2 now stands for the AOT head protons (the influence of the other protons is negligible, as shown in the last section). With the relaxation rates of the polar head protons considerably higher than those of water, one can set $M_2 = M_{20}$ in eq 7 when observing the water magnetization M_1. The "outside" relaxation is then given by R_{11} in (8). In order to use eq 8, some assumptions about the movements in the system are needed, and a simplified model must be used.

(a) As for the "inside" relaxation, we suppose that the exchange rate of water between layer and core inside the micelle is fast enough to average the relaxation of water over the whole micelle (this is experimentally supported by the monoexponential relaxation behavior).

(b) As the local effects at small distance now dominate the relaxation (averaging the dipolar interaction over all directions), the slower movements like overall motion cannot be seen; we will then use the simplest expression of the spectral density with one correlation time τ_0, which will integrate the various dynamical processes like rotations, exchanges, etc. Then:[18]

$$(1/T_1)_{out} = (2/5)\gamma^4\hbar^2 I(I+1)N\langle r^{-6}\rangle \times [\tau/3 + \tau/(1+\omega^2\tau^2) + 2\tau/(1+4\omega^2\tau^2)] \quad (13)$$

where N is the number of nuclei which relax the system and r is their distance. The ratio of relaxation rates at two different frequencies ω_1 and ω_2 only depends on the dynamical factors $X = (\omega_1\tau_0)^2$ and $F = (\omega_2/\omega_1)^2$:

$$(1/T_1)_2/(1/T_1)_1 = \frac{1 + 3/(1+XF) + 6/(1+4XF)}{1 + 3/(1+X) + 6/(1+4X)} \quad (14)$$

Using this relation to fit the ratios of the relaxation rates at 60 and 250 MHz, the correlation times τ_0 were calculated as listed in Table III (the contribution of aliphatic protons evaluated in the last section was previously substracted from the experimental data). Using eq 19, values for $N\langle r^{-6}\rangle$ were extracted. To get an average value of r we used $N = 3$ which seems reasonable in our case. The results are also listed in Table IV. (It must be pointed out that for $W = 15$ the interpolation process to get "outside" contributions led to such small values that they gave an estimated 50% inaccuracy on the correlation time.)

r_{eff} is in the range of typical effective mean distances between protons and increases with W as expected. On the other hand, the typical values for τ_0 (about 5×10^{-10} s) fall between two main correlation times: that of water molecules (10^{-11} s) and of the whole aggregate (5×10^{-9} s). This is consistent with our description of water/polar head interactions. τ_0 can be considered as the lifetime for water absorption in the layer, or alternatively as the diffusion time of water molecules from the polar heads, or as any combination of similar movements.

Trying a more involved approach, one can ask what are the physicochemical processes from which the movements derive. The most important interactions involving water molecules in the micelle are mutual exclusion between components (van der Waals or hard-sphere interactions); hydrogen bonds with water molecules or AOT ester groups; and electrical interactions with the ions. In bulk ionic solutions of Na^+,HSO_3^- the global action of these three interactions is summarized by the "structure-forming" effects.[19] The water molecules form a shell of higher order and cohesion around the ions than in pure water; among other consequences their slower motions increase the NMR relaxation rate of water. In a similar way, the nature of the ions in the micelle

(19) Hertz, H. G. In *Water, a Comprehensive Treatise*; Franks, F., Ed.; Plenum: New York, 1973; Vol. 3, Chapter 7.
(20) Assih, T.; Larché, F.; Delord P. *J. Colloid Interface Sci.* **1982**, *89*, 35.
(21) Atik, S. S.; Thomas, J. K. *J. Am. Chem. Soc.* **1981**, *103*, 3543.

as well as the "inside" relaxation rate values confirm the existence of structure-forming effects in the system. This is not obvious, since in bulk solutions the structure-forming effects are due in part to stronger rearranged hydrogen bonds around the solute molecules, whereas in the AOT inverse micelles, the hydrogen bond rate (as given by the proton chemical shift[6]) is known to be lower than in pure water. Thus the other competitive molecular interactions must be seen as responsible for the observed structure-forming effects. The "outside" relaxation is induced when the water molecules are in the hydration shell of the SO_3^- groups, or hydrogen bonded to the ester groups, both close to the AOT polar head protons. τ_0 could then be seen as a lifetime for water in the AOT polar head hydration shell.

Conclusions

The molecular movements of water in reversed ionic micelles were clarified. The individual motions were shown to be very similar, even at very low water content, to those found in bulk concentrated ionic solutions. As in bulk water, the rotational and translational diffusions as well as the hydrogen exchanges could not be distinguished. The correlation time is then a mixture of various contributions of the same order of magnitude.

A qualitative picture of water–polar head interactions could be drawn. The amount of water molecules adsorbed on the polar heads is about four molecules per AOT molecule; the characteristic correlation time of the water–polar head interaction is in the 5 $\times 10^{-10}$ s range.

Besides, the experiment showed the need of an appropriate methodology to avoid misleading interpretations of NMR relaxation experiments in microheterogeneous systems where many nuclear interactions and movements occur simultaneously. However, this complexity can become a source of small-scale dynamical informations on these systems.

For further studies of water in reversed micelles, surfactants other than AOT should be used. The complexity of its polar head does not allow one to draw simple conclusions expandable to other surfactants, while its chemical instability and complex purification procedure can lead to experiments of low reliability and reproducibility.

Acknowledgment. The authors acknowledge several collegues for help or discussions. We primarily thank A. Lowenstein, J. Tabony, and one of the referees for constructive criticism of the interpretation, and M.-P. Pilēni and J.-F. Le Marēchal for help with the chemistry.

Appendix

To derive eq 9 to 11 in section b, we must integrate the dipolar spectral density for an isolated pair of protons over the core and shell distributions of protons. Because of the motion peculiarities in the shell (assumption f), the shell protons are confined on the surfaces of concentric spheres (of radii $R \geq R_2$), whereas the core protons diffuse inside a sphere (of radius R_1). The two-particle spectral density in this case, which can be found elsewhere,[15,16] is a series of Lorentzian functions:

$$J(\omega) = 1/R^6 \sum_{l,\, n=0}^{\infty} A_{ln}\tau_{ln}/(1 + \omega^2\tau_{ln}^2) \qquad (15)$$

where the A_{ln} are the reduced amplitudes:

$$A_{ln} = [(2l + 3)(l + 2)(l + 1)l^2]/[u_{ln}^2(u_{ln}^2 - l(l + 1))] \times (R_1/R)^{2l}/4\pi \qquad (16)$$

$$A_{00} = 1/4\pi$$

and where the correlation times and the u_{ln} constants are given in eq 11 and 12.

For shell over core relaxation (J_1 in coefficients R_{11} and R_{12}), J must be integrated over R, with particle density N_2. Since R does not appear in the Lorentzian functions, the amplitudes integrations yield:

$$\int_{R_2}^{R_a} (A_{ln}/R^6)4\pi N_2 R^2\, dR = N_2/R_2^3 B_{ln} \qquad (17)$$

The explicit expression found for B_{ln} is given by eq 10.

For core over shell relaxation (J_2 in R_{21} and R_{22}), J must be multiplied by the number of core protons, $2NW$. The spectral density is then a function of R which labels the site distribution in the shell. Since the shell protons are aggregated into a single site (assumption j), the spectral density must be averaged over R. Finally the amplitudes averages give:

$$2NW\int_{R_2}^{R_a} (A_{ln}/R^6)4\pi N_2 R^2\, dR/37N = (2W/37)(N_2/R_2^3)B_{ln} \qquad (18)$$

The $37N$ factor is the number of protons in the surfactant shell (there are 37 protons per AOT molecule and N is the aggregation number). The ratio of eq 17 and 18 yields $J_2(\omega)$ as given in expression 9.

Registry No. AOT, 7732-18-5; H_2O, 577-11-7; D_2O, 7789-20-0.

On the Correspondence between Simple Orbital Concepts and Molecular Electron Distributions

Tom S. Slee

Contribution from the Department of Chemistry, McMaster University, Hamilton, Ontario, Canada L8S 4M1. *Received April 23, 1986*

Abstract: It has been shown that definitions of atoms and their properties, bonds, and molecular structure can be obtained from a study of the molecular electron distribution. The charges on the atoms so defined are often close to "chemical intuition", but in some cases there are major differences. This paper clarifies the relationships between "chemical intuition" based on simple orbital arguments and the actual distribution of charge as described by its atomic charges and by the properties of critical points of the electron density (points where the gradient of the density vanishes). Equations are derived which show how changes and trends in critical point positions and properties can be understood in terms of perturbational molecular orbital (PMO) models. The relationship between PMO models and atomic charges is also quantified, and some previously published data are accounted for by using this relationship. Finally, the effects of the fluoro substituent on the ethyl, vinyl, and carbonyl groups are used to illustrate the general results.

The quantum theory of atoms in molecules developed over recent years by Bader and co-workers[1,2] yields definitions of atoms and bonds in molecules from an analysis of the topology, or qualitative form, of molecular electron distributions. The atoms

0002-7863/86/1508-7541$01.50/0